

## Influence of vertical load on in-plane behavior of masonry infilled steel frames

Sayed Mohammad Motovali Emami<sup>a</sup> and Majid Mohammadi\*

*International Institute of Earthquake Engineering and Seismology (IIEES), No. 26, Arghavan St., North Dibajee, Farmanieh, P.O. Box 19395/3913, Tehran, Iran*

*(Received May 26, 2016, Revised September 4, 2016, Accepted September 27, 2016)*

**Abstract.** Results of an experimental program are presented in this paper for the influence of vertical load on the in-plane behavior of masonry infilled steel frames. Five half-scaled single-story, single-bay steel frame specimens were tested under cyclic lateral loading. The specimens included four infilled frames and one bare frame. Two similar specimens as well as the bare frame had moment-resisting steel frames, while the remaining two specimens had pinned steel frames. For each frame type, one specimen was tested under simultaneous vertical and lateral loading, whereas the other was subjected only to lateral loading.

The experimental results show that the vertical load changes the cracking patterns and failure modes of the infill panels. It improves dissipated hysteresis energy and equivalent viscous damping. Global responses of specimens, including stiffness and maximum strength, do not change by vertical loading considerably. Regarding the ductility, the presence of vertical load is ignorable in the specimen with moment-resisting frame. However, it increases the ductility of the infilled pinned frame specimen, leading to an enhancement in the m-factor by at least 2.5 times.

In summary, it is concluded that the influence of the vertical load on the lateral response of infilled frames can be conservatively ignored.

**Keywords:** masonry Infill; vertical load; steel frame; connection rigidity; m-factor

---

### 1. Introduction

Infill walls are usually considered as non-structural members in the seismic provision. They are used to fill steel or concrete frame as interior or exterior partitions. The presence of infills increases the stiffness and strength of the infilled frame in comparison with the bare frames. The interaction between the infill wall and the frame may or may not be beneficial to the seismic behavior of the structure. Although several models (Smith and Carter 1969, Mainstone 1971, El-Dakhkhni *et al.* 2003, Asteris *et al.* 2011, Tarque *et al.* 2015) have been proposed to consider the effects of infill on the structures but these models are not sufficiently reliable. This is due to inherent uncertainty and several effective variables of the infilled frames such as mechanical properties of infill, connection of infill to frame, details of surrounding frame, workmanship and vertical load

---

\*Corresponding author, Assistant Professor, E-mail: [m.mohammadigh@iiees.ac.ir](mailto:m.mohammadigh@iiees.ac.ir)

<sup>a</sup>Ph.D. Candidate, E-mail: [sm.emami@iiees.ac.ir](mailto:sm.emami@iiees.ac.ir)

applied to beam or column of the frame. The models for simulating the in-plane influence of infills can be divided into two major approaches; micro modeling and macro modeling. The micro modeling has been widely studied by many researchers (Asteris 2008, Stavridis and Shing 2010, Asteris *et al.* 2013) and provides acceptable accuracy to predict both linear and nonlinear behavior of infill frames. These models are normally based on finite element method (FEM) and require a lot of computational time as well as many parameters for the calibration (Asteris *et al.* 2013). Another approach for simulating infills in frames comprises replacing the infill with one or more equivalent compression struts (macro model). Mainstone showed that the width of equivalent strut just depends on mechanical properties of the infill and the frame. The equivalent strut has the same mechanical properties and thickness of the infill. Its width depends on the contact length of the infill to the frame. The vertical load affects behavior of infilled frames by changing the contact length of the infill to the frame (Campione *et al.* 2014). However, most of the macro models have been developed based on experimental results, in which the vertical loads were not considered. Some researchers studied the influence of vertical load, including the gravity load on top beam of the frame as well as axial loads of the columns, on the behavior of infilled frames. Regarding the influence of columns axial loads, Valiasis and Stylianides (1989) carried out some experimental tests on 1/3 scaled RC frames with brick masonry infills. They observed that the presence of axial load on the column improves the in-plane strength of the infilled frames. Some researchers studied the effects of vertical load on the in-plane behavior of infilled frames. Stafford Smith (1968) investigates the effect of vertical loading on the lateral stiffness and strength of concrete infills surrounded by steel frames. The applied vertical load was distributed on the top beam of the infilled frames. He found out that the lateral strength and stiffness of the infilled frames are increased by applying vertical load which is lower than half of compressive strength of the infill panels. Nevertheless higher levels of vertical load have adverse effect on the behavior of the system. Lafuente *et al.* (2000) conducted ten half scaled tests on masonry walls surrounded by minor reinforced concrete frames. The specimens were subjected to combined vertical and cyclic lateral loading. The vertical load was imposed to top beam of the specimens. The amounts of vertical load were equal to 5%, 7.5%, 10% and 15% of infill compressive strength. The results showed that the maximum increase in lateral strength (90%) as a consequence of applying vertical load occurs under vertical load equal to 10% of infill compressive strength. Mehrabi *et al.* (1996) conducted some experimental tests on reinforced concrete frames with masonry infill panels. It can be inferred from this study that the distribution of the vertical load between the columns and the top beam is not important. Also, they found out that an increase of 50% in vertical load results in 25% and 30% improvement in the strength and initial stiffness, respectively. Liu and Manesh (2013) carried out an experimental investigation on concrete masonry infilled steel frames subjected to combined lateral and axial loading. This study has shown that the presence of axial load results in a considerable increase in the lateral strength of infilled frames. Based on this study, the ductility of the infilled frame is improved by applying the axial load which is less than 10% of infill compressive strength.

To consider the influence of vertical load on the behavior of the infilled frames, Asteris *et al.* (2015) and Campione *et al.* (2014) have tried to modify the strut width. In these studies, it is assumed that the vertical load is applied only on the columns of infilled reinforced concrete frames. As a result of their studies, they proposed analytical curves to modify strut width for different vertical load levels.

Despite the abovementioned studies, a firm conclusion cannot be drawn about the influence of vertical load on the behavior of infill panels. Therefore, this paper is devoted to investigate this

subject more, especially on the in-plane behavior of steel frames having rigid or even pinned connections of beams to columns. Five half-scaled frame specimens were tested by applying the lateral cyclic loading on the roof level and constant vertical load on the top beam. The amount of vertical load was considered 10% of compressive strength of infill panel. The in-plane responses, equivalent viscous damping, normalized cumulative energy as well as the component capacity modification factor (m-factors) (ASCE41-06 (2006), ASCE41-13 (2012)) of the specimens are assessed and compared for the effect of vertical loading.

## 2. Experimental work

### 2.1 Test specimens

A four-story, three-bay steel structure was selected as the prototype. The structure was analyzed and designed according to the Iranian seismic code of practice No.2800 (2005) and AISC-ASD89 (1989) steel code of practice. The live and dead loads were taken as 2 and 6 kN/m<sup>2</sup>, respectively. The middle span of the first story of the structure was selected and scaled to 1/2 for the frame of the specimens.

Five specimens consisted of three moment-resisting steel frames and two pinned steel frames were tested under reversed lateral cyclic loading. In the former, the frames had rigid beam-column connections, while in the latter the frames had pinned beam-column connections. The frames were single-story single-bay with 1.5 m height and 2.25 m length (length to height ratio of 1.5). The thickness of the infill panels was 100 mm. IPBL120 and IPBL180 sections were used for the beams and columns of the frames, respectively. IPBL120 section had area of 2530 mm<sup>2</sup> and the second moment inertia of 6.06×10<sup>6</sup> mm<sup>4</sup>. IPBL180 section had area and second moment inertia of 4530 mm<sup>2</sup> and 2.51×10<sup>7</sup> mm<sup>4</sup>, respectively. Two 100×120×6 mm plates connected two sides of the beams web to the columns to provide the pinned connections in the pinned frames.

According to the Iranian National Building code-part 8 (2005) the brick masonry units were pre-soak before using for the construction of the infills. This process improved the bond strength of the mortar-brick interface. All joints of the wall (including horizontal and vertical joints) were filled by 10 mm thick mortar. The mortar was also applied to the gaps between the frame and the infill in order to provide a full contact in between.

Table 1 summarizes the overall properties of the specimens. The first column of Table 1 shows the name of the specimens. The bare frame is named BF, while the names of others are consisted of two or three parts. The letter M at the beginning of the names indicates that the material of the infills is masonry (M). The PC or RC represents the type of beam-column connections of the

Table 1 Summary of specimens

Specimen	Column	Beam	Beam to column connection	Vertical load (kN)
BF	IPBL 180	IPBL 120	Rigid	0
M-RC	IPBL 180	IPBL 120	Rigid	0
M-RC-VL	IPBL 180	IPBL 120	Rigid	200
M-PC	IPBL 180	IPBL 120	Pinned	0
M-PC-VL	IPBL 180	IPBL 120	Pinned	200

frame (RC for rigid and PC for pinned connections). Moreover, the specimens having vertical load are demonstrated by VL in the last part of their names.

## 2.2 Test setup

The overall schematic view of the experimental setup, including the specimen, lateral and vertical loading setups and some other details are illustrated in Fig. 1. Each frame had two columns and two beams. The bottom beam was representative of the floor beam of the frame. The lateral load was applied to the specimens by an actuator through high strength CK45 rod. The capacity of the actuator was 500 kN with maximum 150 mm stroke in both negative and positive directions. The assumed directions of the lateral loading which will be applied later to explain the behavior of the specimens are shown in Fig. 1(a). The vertical load was imposed to the top beam of the bounding frame by a hydraulic static jack as shown in Fig. 1(a). One side of the hydraulic jack was connected to a very stiff beam. In other side the vertical load was applied to a stiffened IPB220 beam. The mentioned beam was supported with two roller constraints at its two ends. The

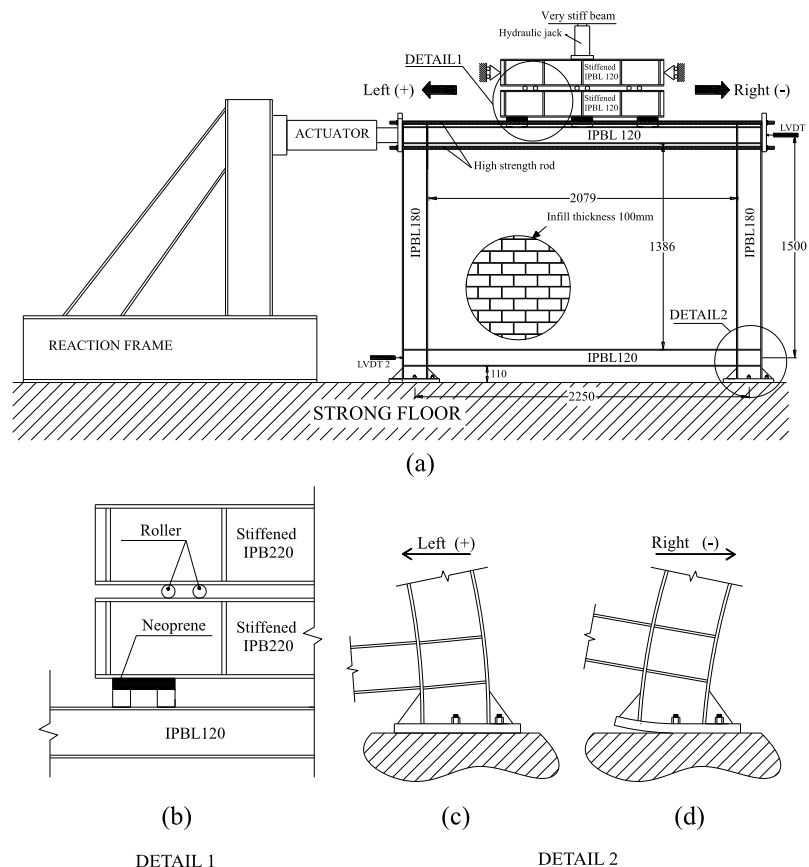


Fig. 1 Test setup: (a) schematic view, dimension in mm; (b) detail of vertical loading setup; (c) rigid connection of column base plate in the positive direction; (d) rotation of base plate when load is applied in the negative direction



Fig. 2 Setup details; (a) vertical loading and out of plane bracing configuration; (b) out of plane bracing view

load was then transferred through three rollers to another stiffened IPB220 beam, which was connected to the top beam of the specimen frame through three 150×100×50 mm neoprene as shown in Fig. 1(b). By this configuration, it could be expected that the vertical load would be uniformly applied to the top beam of the frame at three points. Moreover, this setup allowed the frame to move easily in the left and right directions while imposing the lateral load. A view of the vertical loading setup is depicted in Fig. 2(a). The vertical load was 200 kN, approximately equal to 10% of compressive strength of the infill panel. This load remained constant during testing. An out of plane bracing system was provided to prevent out of plane movement of the frame during testing, depicted in Fig. 2(b).

Due to the distance between the holes of the bolts on the laboratory strong floor, the columns base plates were regulated in such a way to determine the behavior of specimens for two different types of base plates. The base plate is fixed when the specimen is loaded in positive direction but it can rotate when it is loaded in negative direction, as shown schematically in Figs.1(c)-(d).

Relative lateral displacement of the specimens was measured by using two LVDTs installed along the top and bottom beams of the frame, as shown in Fig. 1(a).

### 2.3 Material properties

All infill walls of the specimens were constructed by an experienced mason to minimize workmanship effects. As mentioned before, the solid unit bricks were pre-soaked before using for construction. For all specimens an identical ratio of sand to cement volume (6:1) was used to make mortar. Twelve 50×50×50 mm mortar specimens were made and tested to measure the compressive strength according to ASTM C-109 (2002). The average compressive strength of the mortar specimen was obtained 8.3 MPa with standard deviation of 1.2 MPa. During the infill construction, some standard masonry prisms were made. The prism specimens had the same curing of the wall and were tested in the same time of the infill specimens testing. Each prism included three brick units and two layers of mortar in which the height to thickness was 2. The average compressive strength and module of elasticity of 15 masonry prisms, measured based on ASTM C1314 (2004), were obtained as 9.5 MPa and 1710 MPa, respectively. The material properties of steel sections were obtained by testing 6 coupon specimens. These specimens were provided from

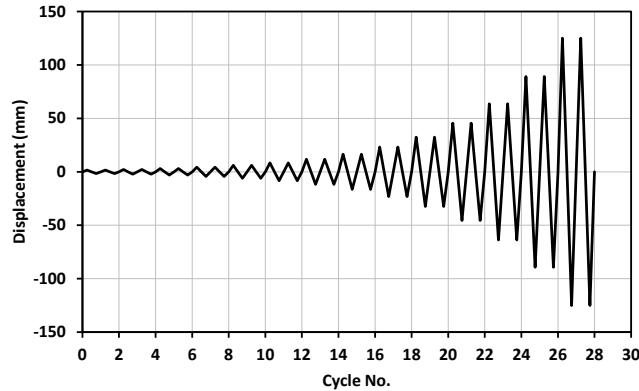


Fig. 3 Applied displacement history

the beam and column sections. The mean values of yield stress, ultimate stress and modulus of elasticity of the steel were 313, 485 MPa and 182.815 GPa, respectively, measured based on ASTM E8/E8M (2009).

#### 2.4 Loading protocol

Displacement control loading pattern recommended by FEMA461 (2007) was applied to the infill specimens, shown in Fig. 3; the amplitude of the first cycle was 1.6 mm. Each cycle was repeated twice and gradually increased by a factor of 1.4. The amplitude of the last cycle was 125 mm which was approximately corresponding to the drift of 8%. The displacement velocity at the first cycles of the test was 1 mm/s and gradually reached to 2 mm/s at last cycles to ensure that the lateral loading imposed to the specimens can be assumed as static. The loading was continued to reach 125 mm lateral displacement or to occur a severe damage in the specimen

### 3. Experimental results

#### 3.1 Specimen BF

The first specimen was bare moment-resisting steel frame. The obtained hysteresis behavior is shown in Fig. 4. The calculated initial stiffness was 9.5 kN/mm and 7.45 kN/mm in the positive and negative loading directions, respectively. The yielding of the specimen was started at the drift of 1.7%. At this displacement, the plastic hinge was developed at the flange of columns base and at the two ends of beams. This was visually obvious through the spalling of lime coating. The maximum lateral strength was 254 kN in the positive direction and 215 kN in the negative direction, which both occurred at the drift of 3.6%. Afterward, the load was reduced and the test was terminated due to the damage in beam-column connection and subsequently failure of it. It should be noted that the difference of the stiffness or the strength between positive and negative directions is attributed to the rigidity difference of columns base plates, as depicted in Figs. 1(c)-(d); at the positive direction the base plates is approximately rigid, while in the negative direction the base plates can rotated.

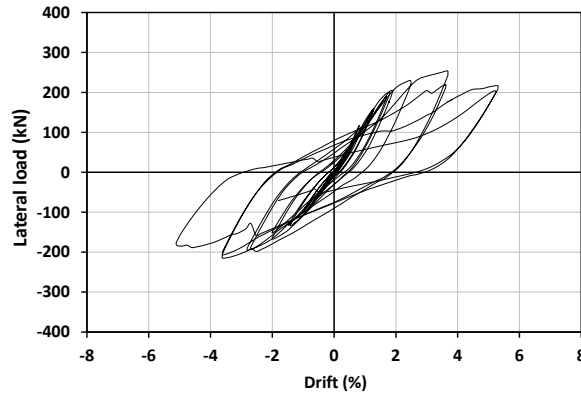


Fig. 4 Lateral load-drift relation for specimen BF

### 3.2 Specimen M-RC

Specimen M-RC, considered as the reference specimen, was a moment-resisting steel frame (had rigid beam-column connections) with brick masonry infill panel. The load-displacement curve of specimen M-RC is depicted in Fig. 5. The stiffness of the infill specimens remained almost constant after occurrence of interface cracking up to drift corresponded to infill cracking. This stiffness is named as practical stiffness. In summary, the practical stiffness is the slope of a line tangent to the load-displacement envelope curve after the occurrence of interface cracking, proposed by Mohammadi (2007), as illustrated in Fig. 6. The practical stiffness of the specimen was 10.6 kN/mm and 8.4 kN/mm in positive and negative directions, respectively. The maximum strength of the specimen was 325 kN at the drift of 5.1% in the positive direction of loading, however it was 218 kN at the drift of 3.5% in the opposite direction of loading. During the testing, the first cracking was initiated at the drift of 0.23% in mortar joints. The cracking pattern of the specimen in both positive and negative directions of loading is presented in Fig. 7; cracks in larger amplitude are shown in darker color. The inclined cracks indicate that two off-diagonal compression struts were formed in the infill panel in each direction.

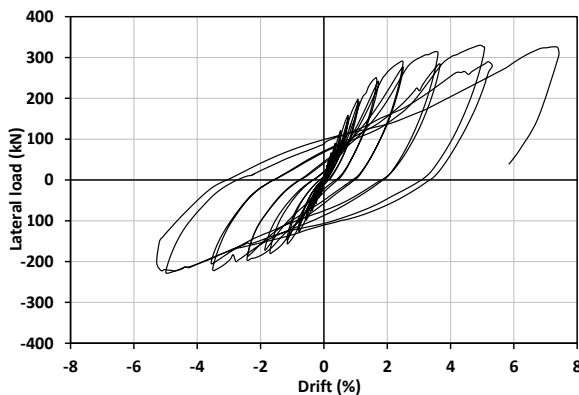


Fig. 5 Lateral load-drift relation for specimen M-RC

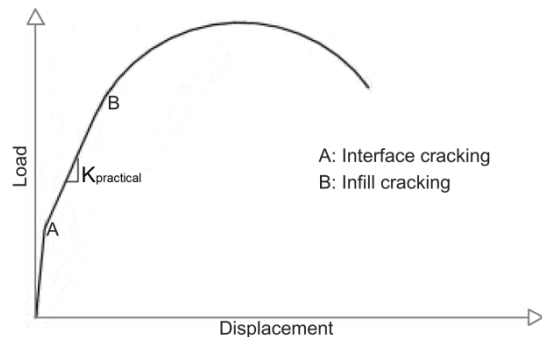


Fig. 6 Practical stiffness of infilled frames

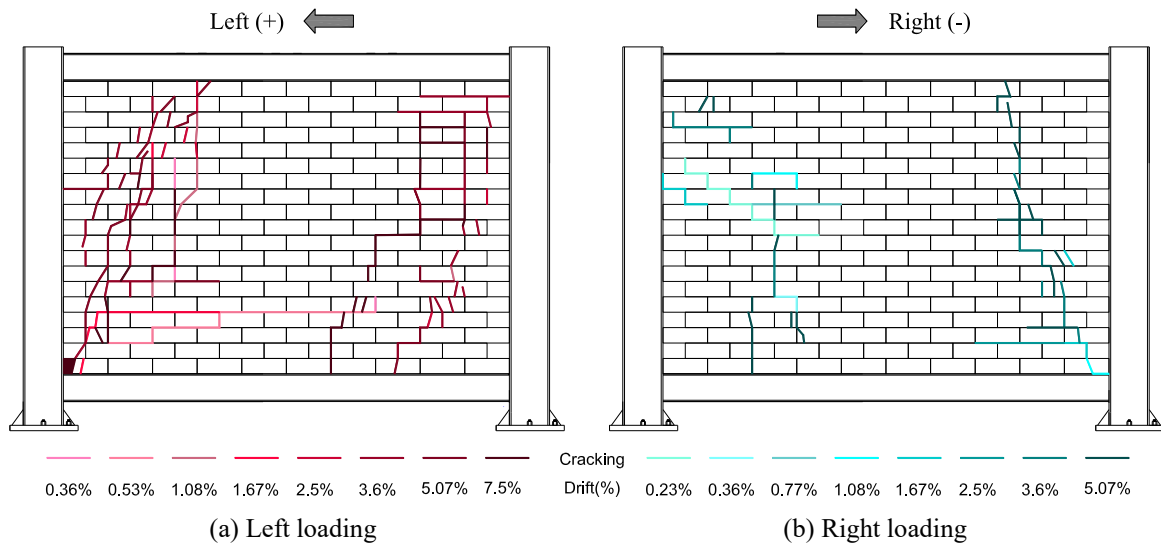


Fig. 7 Cracking pattern in specimen M-RC corresponding to lateral drift (cracks in greater drift are shown in darker color)

No corner crushing or severe damage was observed in the specimen. The test was stopped at the drift of 7.4%, due to out of plane movement of the specimen in the negative direction. This event has exacerbated the difference between the strength of positive and negative directions in this specimen.

### 3.3 Specimen M-RC-VL

This specimen was similar to specimen M-RC, but 20 ton vertical load was applied to the top beam of the specimen. The vertical load had been imposed before applying the lateral load. The load-drift relationship is shown in Fig. 8. The practical stiffness was measured 8.4 kN/mm and 6.5 kN/mm in the positive and negative directions of loading, respectively, which were both slightly

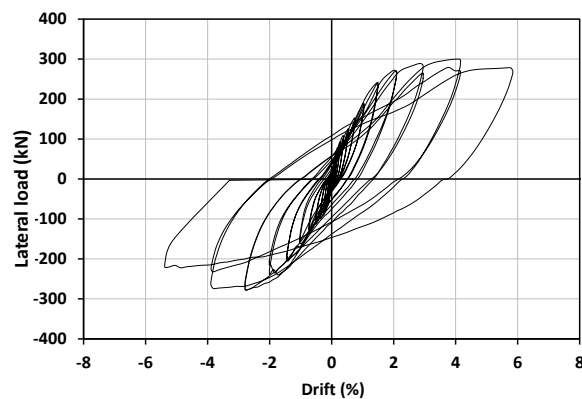


Fig. 8 Lateral load-drift relation for specimen M-RC-VL

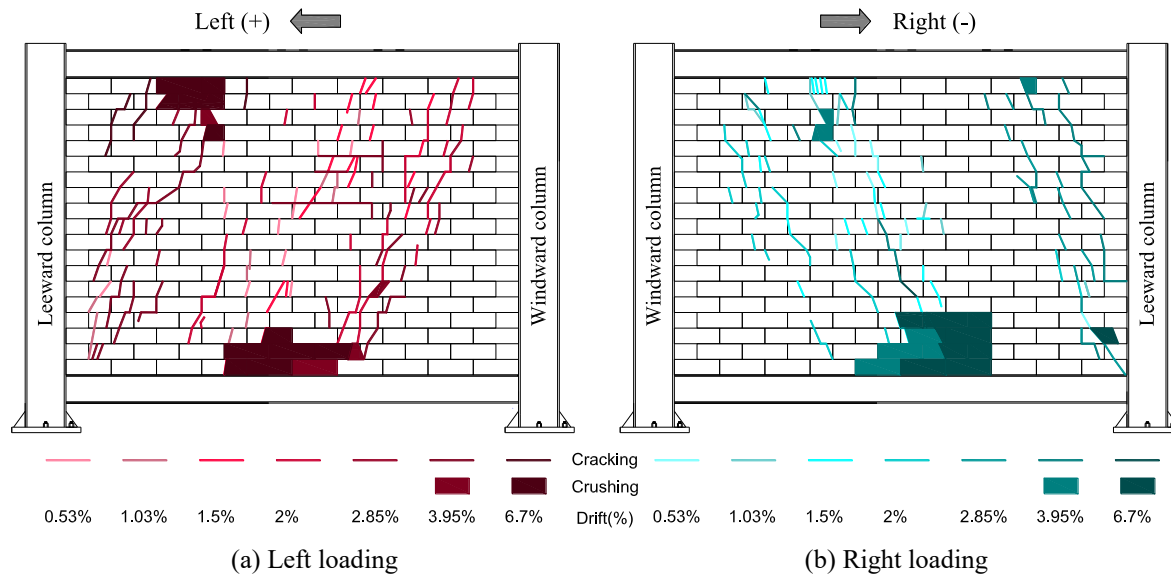


Fig. 9 Cracking pattern and crushing in specimen M-RC-VL corresponding to lateral drift (cracks in greater drift are shown in darker color)



Fig. 10 Failure mode of specimen M-RC-VL

lower than stiffness of specimen M-RC. The peak load was 300 kN occurred at the drift of 3.95% in the positive direction and 278 kN at the drift of 2.8% in the negative direction. The first crack was developed almost vertically in the middle part of the infill panel as opposed to specimen M-RC. By increasing the lateral amplitude, the cracks began to shift to the leeward column. The cracking pattern of specimen M-RC-VL is shown in Fig. 9; two compression struts can be observed in each direction of loading similar to specimen M-RC, which one of them has obviously greater width. Having more cracks in the middle part of the infill panel in comparison with specimen M-RC may be attributed to the applied vertical load on the top beam. The test was

stopped at the drift of 5.7% in which some bricks were completely crushed and lead to decrease in lateral strength. The failure mode of the specimen is depicted in Fig. 10.

### 3.4 Specimen M-PC

This specimen was a masonry infilled pinned frame, in which the bounding frame had pinned beam-column connections. The load-drift relationship of the specimen is shown in Fig. 11. The calculated practical stiffness in positive and negative directions was  $\text{kN/mm}$  5.6 and  $3.6 \text{ kN/mm}$ , respectively. The peak load was 290 kN in the positive direction and 185 kN in the opposite direction. During the testing, the interface cracking was occurred at very small drift of 0.05%. The hairline cracks were initiated along the horizontal and vertical mortar joints at the drift of 0.16%. As the drift increased, the inclined cracks were developed in the bricks. The cracks of the specimen according to their corresponding drifts are shown in Fig. 12. One can observe that similar to specimen M-RC, two inclined compression struts have been developed. At the drift of 3.5% the beam-column connections started damaging and subsequently the test was terminated at the drift of 5.5% for the failure of top beam connections.

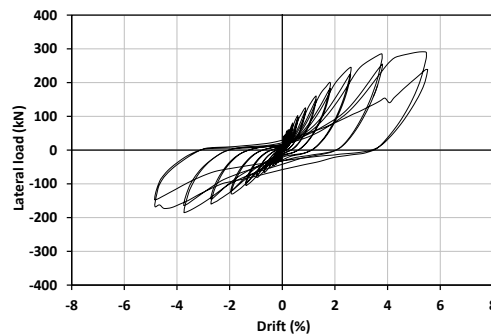


Fig. 11 Lateral load-drift relation for specimen M-PC

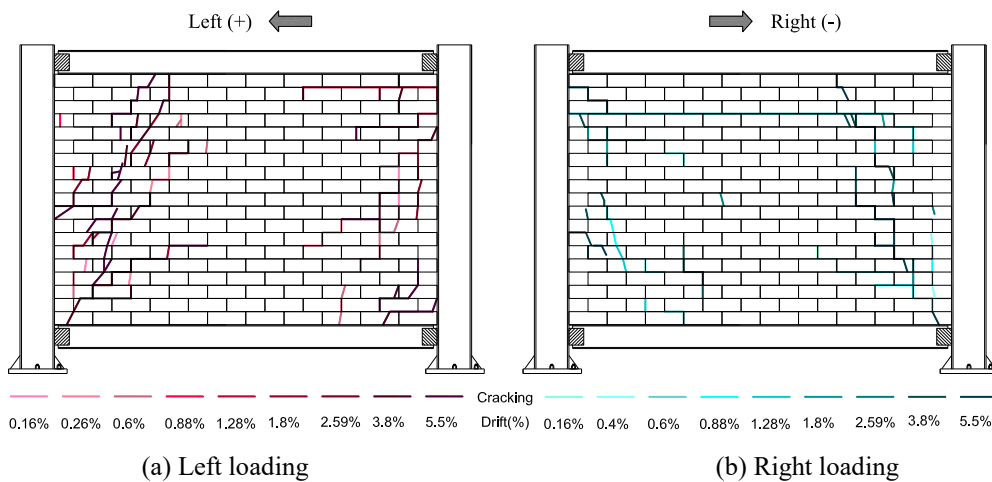


Fig. 12 Crack pattern in specimen M-PC corresponding to lateral drift (cracks in greater drift are shown in darker color)

### 3.5 Specimen M-PC-VL

The last specimen was a pinned steel frame with masonry infill panel similar to specimen M-PC but under combined lateral and vertical loading. The hysteresis curve of the specimen is illustrated in Fig. 13. The practical stiffness was measured as 6.8 and 5.4 kN/mm in the positive and negative directions, respectively. The peak load was 274 kN at the drift of 2.8%, in the positive direction and then dropped to 220 kN in the next cycle of loading at the drift of 5.6%. In the negative direction, the peak load was 191 kN and gradually decreased to 154 kN at the drift of 5.4% in the next two cycles of loading. The cracking pattern is shown in Fig. 14. Similar to specimen M-RC-VL, the first cracks were developed at the middle of the infill, while by increasing the lateral displacement, major inclined cracks gradually shifted to the leeward columns. Subsequently in the drifts greater than 3.9%, some bricks at the top of the infill panel were crushed. Similar to specimen M-PC, the pinned beam-column connection was failed, as shown in Fig. 15, at the drift of 5.6% and consequently the test was terminated.

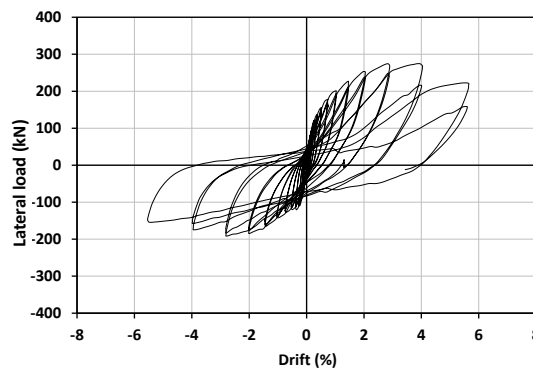


Fig. 13 Lateral load-drift relation for specimen M-PC-VL

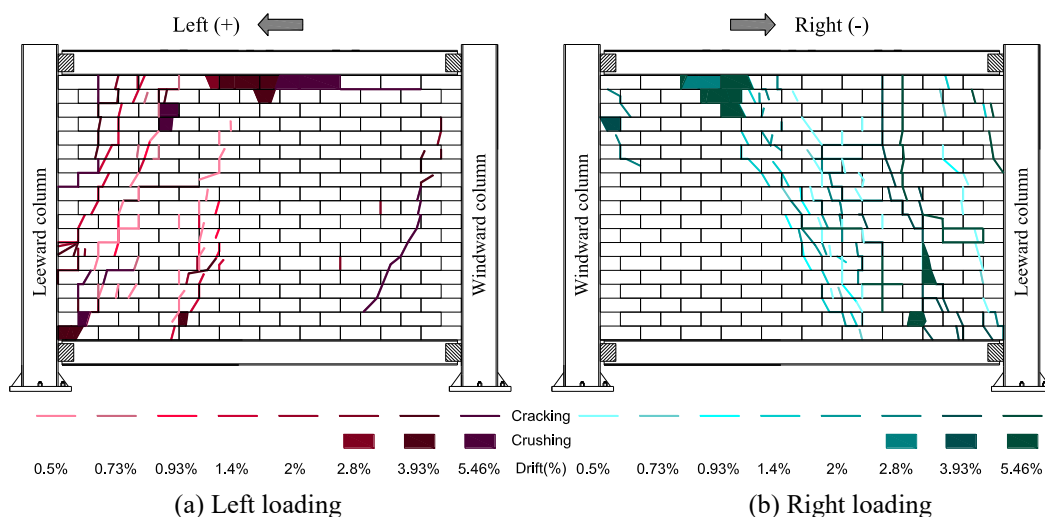


Fig. 14 Cracking pattern and crushing in specimen M-PC-VL corresponding to lateral drift (cracks in greater drift are shown in darker color)



Fig. 15 Failure of pinned connection in specimen M-PC-VL

### 3. Comparison of the test results

Global responses of the specimens are compared in Fig. 16 for hysteresis envelope curves. It can be seen that in all infill specimens compared with the bare frame, the presence of infill improves the in-plane stiffness and lateral strength. The peak load and initial stiffness of specimen M-RC were respectively 3.7 and 1.3 times greater than those of specimen BF in positive direction of loading.

Different types of stiffness and strength as well as their corresponding drifts of the specimens are available in Table 2. The signs + and – indicate the positive and negative directions of loading, respectively. The initial stiffness is taken as the slope of a tangent to the load-displacement curve before interface cracking. The crushing strength (load at major infill cracking) of the specimen with rigid beam-column connections was raised by applying the vertical load. However, the vertical load almost did not change the crushing capacity of the infilled pinned frames. Moreover, the influence of the vertical load on the practical stiffness and maximum strength was not considerable. It should be noted that, the difference between the peak loads of specimens M-RC & M-RC-VL in the negative direction may be attributed to the loss of the strength of specimen M-RC as a consequence of out of plane movement in the negative direction of loading.

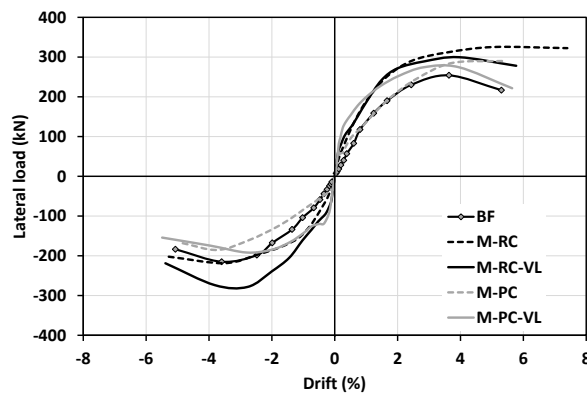


Fig. 16 Lateral load-drift envelopes

Table 2 The important values of strength and stiffness and corresponding drifts of specimens

Specimen	Initial stiffness (kN/mm)	Practical stiffness (kN/mm)	Major infill cracking		Maximum strength	
			Load (kN)	Drift at (%)	load (kN)	Drift (%)
BF	9.5	-	-	-	254	3.63
	7.44	-	-	-	-215	-2.6
M-RC	35	10.6	197	1.07	325	5.07
	-39	-8.4	-125	-0.79	-218	-3.5
M-RC-VL	40.8	8.4	242	1.49	300	3.95
	-35.7	-6.5	-200	-1.45	-278	-2.77
M-PC	52	5.6	200	1.8	290.2	5.46
	-29	-3.6	-130	-1.9	-185.3	-3.72
M-PC-VL	43.5	6.8	201	1.03	274	2.83
	-33.3	-5.4	-142	-0.98	-191.8	-2.8

Energy dissipation of the specimens in term of equivalent viscous damping via the imposed lateral drift is illustrated in Fig. 17(a). The equivalent viscous damping can be calculated as:  $\xi_{eq} = E_D / (4\pi E_S)$ , where  $E_D$  is the amount of energy dissipated by the infilled frame in a completed cycle which is equal to the area enclosed by the load-displacement curve in each cycle and  $E_S$  is the amount of elastic strain energy stored in the same cycle, defined as the half of the maximum displacement multiply by the corresponding load. More details regarding the mentioned formulation can be found in (Chopra 2001, Motovali Emami and Mohammadi 2015). According to the Fig. 17(a), it can be seen that specimen BF has the minimum damping ratio at the beginning, however it is higher than that of specimens M-RC and M-PC after the drift of 2% and remains constant after the drift of 3.5%. The last one may be attributed to the beam-column connection failure of specimen BF after the drift of 3.5%, as point out earlier. In the case of the specimens under combined lateral and vertical loading, the equivalent viscous damping is initially decreased as imposed displacement increased up to the drift of 1% and 1.5% for specimens M-RC-VL and M-PC-VL, respectively. Afterward, the damping ratio is gradually increased, especially in the case of specimen M-RC-VL. Moreover, it is evident that the damping ratio of the specimens under combined lateral and vertical loading, is more than that of in the specimens subjected to lateral load only in throughout the imposed lateral displacement. This is more obvious in the specimens with rigid beam-column connections in the drift values higher than 4%. It may be attributed to the occurring of more cracks in the infill of specimens subjected to combined lateral and vertical loading.

In order to evaluate the amount of the energy dissipated in each cycle, the energy normalized to the peak-to-peak displacement against the imposed lateral drift for the specimens is drawn in Fig. 17(b). This approach was previously utilized by some researchers such as Kakaletsis and Karayannis (2008), Tasnimi and Mohebkhah (2011). From the Fig. 17(b), it can be concluded that the normalized dissipated energy in specimens BF is less than that of specimen M-RC. Similar to the equivalent viscous damping, the normalized energy dissipation per cycle in the specimens imposed to combined lateral and vertical loading is more than that of in the specimens under lateral load only (regardless the type of surrounding frames). As pointed out earlier, it is due to the

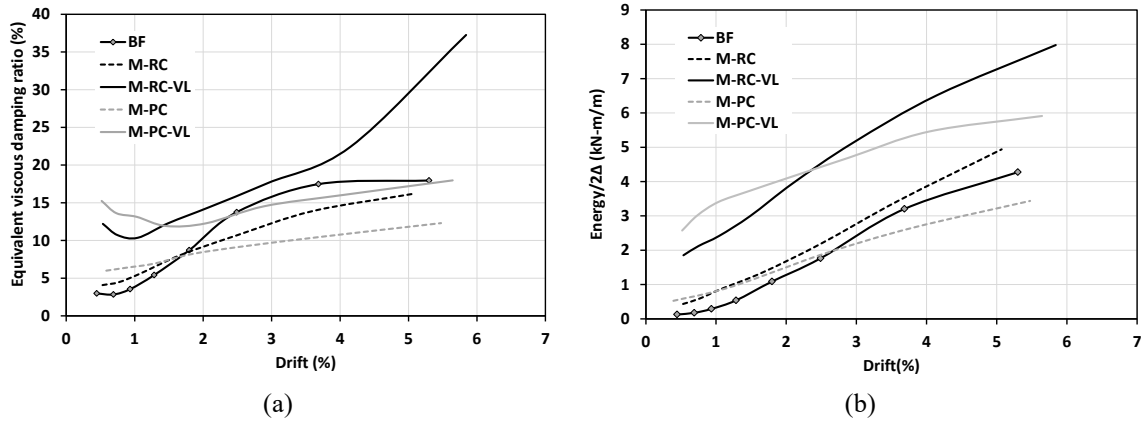


Fig. 17 Comparison of (a) equivalent viscous damping ratio; (b) energy dissipation to displacement ( $2\Delta$ ) per cycle

occurring of more cracks in the infill of specimens subjected to combined lateral and vertical loading than the infill of specimens under lateral load only.

#### 4. Additional analytical investigation

In this section, more investigation is performed to find out the influence of vertical load on the in-plane performance of infilled steel frames. For this reason, parameters of the infilled frames needed for doing linear analysis were computed and compared. In seismic guidelines such as FEMA356 (2000) and ASCE41-13 (2012), infilled frames are considered as Deformation-Controlled elements. For linear analysis of such elements, two essential parameters,  $m$ -factor and  $Q_{CE}$  are needed. The former is the “component capacity modification factor for expected ductility at desired performance level” which can be representative of component ductility and the latter is the expected strength of the element for deformation-controlled action. For deformation-controlled action, the element or component must satisfy Eq. (1)

$$m \times \kappa \times Q_{CE} \geq Q_{UD} \quad (1)$$

Where,  $Q_{UD}$  is the load caused by gravity and earthquake forces and  $\kappa$  is the knowledge factor (ASCE-41-13 (2012)), which is assumed to be 1.0 in this study. In the following, the  $m$ -factors and expected strengths ( $Q_{CE}$ ) of the infilled frame specimens are calculated and compared in order to have a better evaluation of vertical load effects.

The parameters of acceptance criteria were estimated via the idealized backbone curve. The idealized curve should be derived from backbone of load-displacement hysteresis curves. Generally, there are two methods of obtaining backbone curve from experimental hysteresis data;

1- The backbone curve shall be drawn through the intersection of first cycle curve for  $i$ -th amplitude step with the second cycle curve of the  $(i-1)$ -th deformation step for all  $i$  step, recommended by ASCE41-06 (2006).

2- The backbone curve could be extracted through the points corresponding to the maximum displacements of the first cycle of each increment of loading, proposed by ASCE-41-13 (2012).

In this research, the backbone curves obtained through the two above-mentioned methods are referred to as Method1 and Method2 respectively. The backbone curve can be drawn for each direction of loading. Fig. 18(a) illustrates the backbone curves of specimen M-RC-VL derived from hysteresis curve in each direction of loading for the two mentioned methods.

The backbone curve should be converted to an idealized multi-line curve, before calculating the m-factor and  $Q_{CE}$ . There are various methods to idealize the backbone curve (ASCE41-06 2006, ASCE-41-13 2012, Tomazevic 1999). In this study, the recommended method of ASCE41-13 is applied and summarized as follows: the first line of idealized relationship starts from the origin with a slope equal to effective lateral stiffness,  $K_e$ . The effective lateral stiffness,  $K_e$ , is calculated as the secant stiffness at base shear corresponding to 60% of expected strengths ( $Q_{CE}$ ). The expected strength shall not be taken greater than maximum strength at any point along the backbone curve (ASCE-41-13 (2012)). The second line which has positive slope is determined by a point corresponding to the target displacement and another point at the intersection with first line such that the areas below the idealized and backbone curve become approximately equal. The target displacement was taken as the displacement corresponding to the maximum strength. It should be noted that the method of developing the idealized backbone curve require graphical or computational iterations. For example, the idealized curve corresponding to Method2 backbone curve of specimen M-RC-VL is illustrated in Fig. 18(b).

The m-factor was calculated for Life Safety (LS) performance level which can be estimated by  $0.75^2 \times \Delta u / \Delta y$  (ASCE41-06 (2006), ASCE41-13 (2012)). The  $\Delta_u$  and  $\Delta_y$  are displacements corresponding to ultimate and yielding strength, respectively as illustrated in Fig. 18(b). Table 3 reveals the parameters of linear analysis of the infill specimens. The parameters were not calculated for specimen M-RC in negative direction of loading, due to unreliable results caused by out of plane movement of the specimen.

Considering the results shown in Table 3, there is significant difference between the  $m \times Q_{CE}$  of the specimens with pinned connections (M-PC and M-PC-VL), as a result of applying the vertical load. Nevertheless, this difference is marginal for the specimens with rigid connections (M-RC and M-RC-VL). Furthermore, in these specimens, the  $Q_{CE}$  is not considerably changed by applying

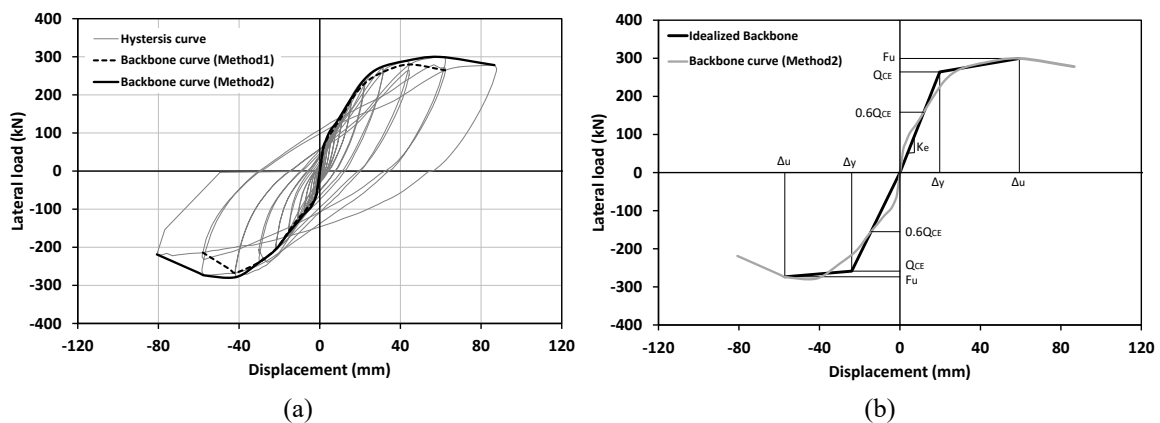


Fig. 18 (a) Backbone curves of specimen M-RC-VL; (b) Idealized of backbone curve (Method2) of specimen M-RC-VL

Table 3 The parameters of linear analysis obtained from experimental data

Specimen	<i>m-factor</i>		$Q_{CE}$ (kN)		$m \times Q_{CE}$ (kN)	
	Method1	Method2	Method1	Method2	Method1	Method2
M-RC	1.7	2.2	226.4	263.1	379.6	590.6
	N.C.	N.C.	N.C.	N.C.	N.C.	N.C.
M-RC-VL	1.4	1.7	231.3	264.1	331.7	446.4
	1.4	1.3	-201.5	-258.6	-283.5	-347.3
M-PC	1.9	1.5	160.2	254.3	308.8	394.1
	1.4	2.1	-117.9	-103.7	-165.4	-217.1
M-PC-VL	4.8	4.7	168.8	210.2	810.9	982.3
	5.2	6.3	-118.8	-136.7	-620	-865.8

the vertical load. Whereas, the maximum difference between the  $Q_{CE}$  of specimens M-PC and M-PC-VL is observed as 32% in negative direction (comparing -136.7 with -103.7). Regarding the *m-factor*, the presence of the vertical load causes an increase from 250% (comparing 4.8 with 1.9) to 372% (comparing 5.2 with 1.4) in the specimens with pinned connections, while it decreases slightly in the specimens with rigid connections. Therefore, it can be concluded that for the infilled moment-resisting frame specimens, the application of vertical load has negligible effects on the parameters of linear analysis. However, it is beneficial for the infilled pinned frame specimens which lead to increase of the *m-factor* by at least 2.5 times.

The same conclusion can be drawn based on results of Liu and Manesh study (2013). Four masonry infilled steel frame specimens F-0, CF-1, CF-2 and CF-3 were selected. These specimens had vertical loads about 0%, 6.6%, 10% and 15% of the infill axial strength, respectively. The vertical load was imposed on the top beam of the specimens and the lateral load was applied monotonically. For more details one can refer to Liu and Manesh study (2013). The *m-factor* and  $Q_{CE}$  of the specimens were calculated based on above-mentioned method (shown in Table 4).

As it can be observed in Table 4, the expected capacity is raised slightly by increasing the vertical load, however, the *m-factor* is not always increased. For example, the *m-factor* of specimen CF-1 (vertical load equal to 15% of axial infill strength) is less than that of specimen F-0 (without vertical load). Regarding the  $m \times Q_{CE}$ , it can be seen that the application of vertical load up to 10% of axial infill strength is beneficial. However, greater vertical loads result in even negative effect on the behavior of infilled frames.

Table 4 The parameters of linear analysis obtained from experimental data of reference (Liu and Manesh study 2013)

Specimen	Vertical load to axial infill strength ratio (%)	<i>m-factor</i>	$Q_{CE}$ (kN)	$m \times Q_{CE}$ (kN)
F-0	0	1.34	115	153
CF-3	6.6	3.71	118	438
CF-2	10	2.47	131	324
CF-1	15	0.79	168	132

In summary, and based on the results of this research it can be concluded that the presence of vertical load up to 10% of compressive infill strength is beneficial, however greater vertical loads should be avoided. It is worth noting that in the regular buildings, the vertical load, including gravity load of wall and slab weight from upper story, is normally less than 10% of infill axial strength. Therefore the presence of vertical load could be normally considered beneficial.

## **5. Conclusions**

In this study, an experimental program was carried out to investigate the effect of vertical load on the in-plane behavior of masonry infilled steel frames. The specimens included four infilled frames and one bare frame. To consider the influence of beam-column connection rigidity of surrounding frame, the infill specimens included two moment-resisting steel frames (with rigid beam-column connections) and two pinned steel frames (with pinned beam-column connections) were tested. In each type of frame, one specimen was imposed under combined lateral and vertical loading and another was subjected only to lateral loading. The vertical load was about 10% of compressive strength of the infill and applied on the top beam of infilled frames. Furthermore, an analytical procedure is carried out to find out if the vertical load has effect on the linear analysis parameters of the infill specimens. The following results can be concluded from this study:

The presence of vertical load changes the infill cracking pattern and failure mode of the specimens, regardless the rigidity of beam-column connections of the frames. The inclined cracks were formed in the specimens without vertical load, while in the specimens having vertical load the cracks were initiated vertically in the middle part of the infill and subsequently, shifted to leeward column.

The practical stiffness and maximum strength of the specimens were slightly affected by the vertical load. However, the equivalent viscous damping and normalized dissipated energy of the infilled frames was increased by applying the vertical load. Comparing linear analysis parameters of the specimens shows that the presence of the vertical load resulted in increase of the m-factor by 2.5 times in the specimen with pinned connections, while it is not considerably changed in the specimen with rigid connections.

In summary, it can be concluded that the application of vertical load up to 10% of the infill compressive strength, causes negligible effects in the major behavior of the infilled moment-resisting frame specimens. However it improves the ductility and consequently the m-factor of the infilled pinned frame specimens.

## **Acknowledgments**

This study was supported financially by International Institute of Earthquake Engineering and Seismology (IIEES), as well as Organization for Renovating, Developing and Equipping Schools of Iran under grant No. 7386 and 7387.

The experimental works were done in the structural laboratory of Structural Engineering Research Centre (SERC) at International Institute of Earthquake Engineering and Seismology (IIEES).

## References

- AISC, ASD (1989), Plastic design specifications for structural steel buildings, American Institute of Steel Construction; Chicago, IL, USA.
- ASCE 41-13 (2012), Seismic rehabilitation of existing buildings, American Society of Civil Engineers; Virginia: Reston.
- ASCE 41-06 (2006), Seismic rehabilitation of existing buildings, American Society of Civil Engineers; Virginia: Reston.
- Asteris, P.G., Antoniou, S.T., Sophianopoulos, D.S. and Chrysostomou, C.Z. (2011), "Mathematical macromodeling of infilled frames: state of the art", *J. Struct. Eng.*, ASCE, **137**(12), 1508-1517.
- Asteris, P.G., Cotsovou, D.M., Chrysostomou, C.Z., Mohebkhah, A. and Al-Chaar, G.K. (2013), "Mathematical micromodeling of infilled frames: state of the art", *Eng. Struct.*, **56**, 1905-1921.
- Asteris, P.G., Cavaleri, L., Trapani, F.D. and Sarhosis, V. (2015), "A macro-modelling approach for the analysis of infilled frame structures considering the effects of openings and vertical loads", *Struct. Infrastruct. Eng.*, **12**(5), 1-16.
- ASTM C109 (2002), Standard test method for compressive strength of hydraulic cement mortars (Using 2-in. or [50-mm] cube specimens), ASTM International West Conshohocken, PA, USA.
- ASTM C1314-03b (2004), Standard test method for compressive strength of masonry prisms, ASTM International, USA.
- ASTM E8/E8M (2009), Standard test methods for tension testing of metallic materials, ASTM international, West Conshohocken PA, USA.
- Campione, G., Cavaleri, L., Macaluso, G. and Amato, G. (2014), "Evaluation of infilled frames: an updated in-plane-stiffness macro-model considering the effects of vertical loads", *Bull. Earthq. Eng.*, **13**(8), 1-17.
- Chopra, A.K. (2001), Dynamics of Structures: Theory and Applications to Earthquake Engineering, Prentice-Hall.
- El-Dakhkhni, W., Elgaaly, M. and Ahmad, A.H. (2003), "Three-strut model for concrete masonry-infilled steel frames", *J. Struct. Eng.*, ASCE, **129**(2), 177-185.
- Federal Emergency Management Agency (FEMA), Prestandard and commentary for the seismic rehabilitation of buildings. Report no. FEMA 356, FEMA, Washington, DC, USA.
- FEMA 461 (2007), Interim testing protocols for determining the seismic performance characteristics of structural and nonstructural components, Federal Emergency Management Agency, USA.
- INBC-Part 8 (2005), Design and construction of masonry buildings, Iranian national building code, part 8, Ministry of Housing and Urban Development, Iran.
- Kakaletsis, D.J. and Karayannis, C.G. (2008), "Influence of masonry strength and openings on infilled R/C frames under cyclic loading", *J. Earthq. Eng.*, **12**(2), 197-221.
- Lafuente, M., Molina, A. and Genatios, C. (2000), "Seismic resistant behavior of minor reinforced concrete frames with masonry infill walls", *Proceedings of the 12th World Conference on Earthquake Engineering*, Auckland, New Zealand, January.
- Liu, Y. and Manesh, P. (2013), "Concrete masonry infilled steel frames subjected to combined in-plane lateral and axial loading-An experimental study", *Eng. Struct.*, **52**, 331-339.
- Mainstone, R.J. (1971), "On the stiffness and strengths of infilled frames", *ICE Proc. Thomas Telford*, **49**(2), 230.
- Mehrabi, A.B., Shing, P.B., Schuller, M.P. and Noland, J.L. (1996), "Experimental evaluation of masonry-infilled RC frames", *J. Struct. Eng.*, ASCE, **122**(3), 228-237.
- Mohammadi, M. (2007), "Stiffness and damping of infilled steel frames", *Proceedings of the ICE-Struct Build.*, **160**(2), 105-118.
- Motovali Emami, S.M. and Mohammadi, M. (2015), "Effect of frame connection rigidity on the behaviour of infilled steel frames", *J. Struct. Eng.*, ASCE (under review).
- Smith, B.S. (1968), "Model test results of vertical and horizontal loading of infilled frames", *ACI J. Proc.*, **65**(8), 618-625.

- Smith, B.S. and Carter, C. (1969), "A method of analysis for infilled frames", *ICE Proc. Thomas Telford*, **44**(1), 31-48.
- Standard No 2800 (2005), Iranian code of practice for seismic resistant design of buildings, Third Revision, Building and Housing Research Center, Iran.
- Tarque, N., Leandro, C., Guido, C. and Enrico, S. (2015), "Masonry infilled frame structures: state-of-the-art review of numerical modeling", *Earthq. Struct.*, **8**(1), 225-251.
- Tasnimi, A.A and Mohebkah, A. (2011), "Investigation on the behavior of brick-infilled steel frames with openings, experimental and analytical", *Eng. Struct.*, **33**(3), 968-980.
- Tomazevic, M. (1999), *Earthquake-resistant Design of Masonry Buildings*, World Scientific.
- Valiasis, T. and Stylianidis, K. (1989), "Masonry infilled R/C frames under horizontal loading experimental results", *Eur. Earthq. Eng.*, **3**(3), 10-20.

CC